



# Corrosion inhibition and adsorption behavior of phytic acid on Pb and Pb–In alloy surfaces in acidic chloride solution

Hany M. Abd El-Lateef<sup>1,2</sup> · Abdel-Rahman El-Sayed<sup>1</sup> · Hossnia S. Mohran<sup>1</sup> · Hoda Abdel Shafy Shilkamy<sup>1</sup>

Received: 11 May 2018 / Accepted: 11 January 2019 / Published online: 2 February 2019  
© The Author(s) 2019

## Abstract

The corrosion and corrosion inhibition of Pb and Pb–In alloys in HCl solution, were investigated. The study was performed in the absence and presence of the phytic acid (PA) inhibitor using potentiodynamic polarization and electrochemical impedance spectroscopy measurements, and complementary by scanning electron microscope (SEM) and X-ray spectroscopy analysis (EDX) investigations. The obtained outcomes showed that the PA is efficient corrosion inhibitor for Pb and Pb–In alloys in HCl solution. The inhibition efficiency ( $\eta$  %) for Pb and its investigated alloys increases with an increase in the concentration of PA and decreases with increasing temperature. The maximum inhibition efficiency ( $\approx 80\%$ ) was obtained at  $1 \times 10^{-3}$  M of the PA inhibitor. Langmuir adsorption isotherm fits well the experimental data. SEM/EDX observations of the electrode surface confirmed the existence of an adsorbed film. One can conclude that the increase in activation energy with increasing additive concentration, in addition to the decrease in  $\eta$  % in the presence of inhibitor with temperature, is suggestive of physical adsorption of the inhibitor molecules on the surface of Pb and Pb–0.5In alloy.

**Keywords** Pb–In alloy · Phytic acid · EIS · Polarization · Acid corrosion

## Introduction

The most important applications of Pb and Pb alloys are of widespread usage in acid storage batteries. The corrosion product films form good mechanical barriers against the environment. However, with long immersion time the depth of layers increases and the crystals become more adherent on the surface [1, 2]. Corrosion process is playing an important role in the field of economics and safety. Hydrochloric acid solutions are used for pickling, chemical and electrochemical etching of metals and alloys [2–4]. Pb forms many alloys, which increases its use in both of industry and daily life. It is well known that alloying content plays an important role in

the improvement of the battery grid properties. Previously, the authors [5] studied the effect of indium alloying with Pb on the mechanical properties and corrosion resistance of Pb–In alloys in sulfuric acid solution. They found that indium alloying with Pb increases its hardness, reduces its electrochemical activity, and improves its stability of corrosion [5]. Acid-induced corrosion is an important and expensive problem in industry and represents a significant portion of loss as a result of lost production, inefficient operation, high maintenance and the cost of corrosion control chemicals. Therefore, study of corrosion inhibition of Pb and Pb alloys in HCl solution is of great importance [6].

The use of inhibitors is considered as one of the most practical approaches for protecting metals against corrosion, especially in acidic media [7]. Many organic compounds were tested and industrially applied as corrosion inhibitors, nontoxic are far more strategic now in recent past. These compounds are adenine, adenosine and 2,4,6-tris(2-pyridyl)-1,3,5-triazine [8–10]. The corrosion inhibition of Pb by different organic compounds has been studied in considerable details [11, 12]. Pyrazol derivatives were found to inhibit the Pb corrosion in acidic chloride solutions, and the inhibition of the corrosion process was explained to be due to the stabilization of  $\text{PbCl}_2$  which is formed as a barrier

**Electronic supplementary material** The online version of this article (<https://doi.org/10.1007/s40090-019-0169-4>) contains supplementary material, which is available to authorized users.

✉ Hany M. Abd El-Lateef  
hmahmed@kfu.edu.sa; Hany\_shubra@yahoo.co.uk

<sup>1</sup> Department of Chemistry, Faculty of Science, Sohag University, Sohag 82524, Egypt

<sup>2</sup> Department of Chemistry, College of Science, King Faisal University, Al Hassa 31982, Saudi Arabia



layer on the metal surface to protect it from continuous corrosion [13, 14]. Unfortunately, some of them are toxic, expensive, and environmentally not safe. The development of eco-friendly corrosion inhibitors with high effectiveness and efficiency is an urgent quest.

The naturally derived materials such as phytic acid and its salts have been used as environmentally being safe corrosion inhibitors [15]. The most attractive advantages of phytic acid include its low-cost and availability as a typically polyphosphorylated carbohydrate [Fig. S1 (supporting data)] is widely found in beans, brown rice, corn, sesame seeds, and wheat bran. Phytic acid is used as cleaning agent, water treatment agent, food additives and cosmetic additive, and has been proved that it is non-toxic to human and “green” to environment [16]. Due to its structure which is containing 12 acid groups, phytic acid and its salts are liable to interact with metal ions to form complexes on the metal surface, acting as antirust and anticorrosive [17–21]. The reaction between active groups of PA and metal ions forms chelate complex compounds, which can deposit on the surface of a metal substrate, and thus improve the corrosion resistance. The literature survey showed that, there are not any data on corrosion behavior of Pb–In alloy in HCl solution. Also, the literature reveals that phytic acid has not almost yet been used as corrosion inhibitor of Pb and its investigated alloys. So, the aim of the present work was to investigate the effect of phytic acid as a green inhibitor on the corrosion behavior of Pb and Pb–In alloys in HCl solution at different temperatures. Corrosion inhibition of Pb and Pb–In alloys in HCl solution in the presence of PA has been studied by potentiodynamic polarization and electrochemical impedance spectroscopy (EIS) techniques complemented with some SEM and EDX observations. The mechanism of inhibition is discussed on the basis of an adsorption isotherm, as well as, the calculated thermodynamic parameters.

## Experimental section

### Materials and solutions

Pb and In of high purity (99.999% Johnson Matthey Chemicals Ltd.) were used to prepare Pb–In alloys as disk electrodes ( $A = 0.196 \text{ cm}^2$ ) in a Gallenkamp muffle furnace using evacuated closed silica tubes at  $500 \text{ }^\circ\text{C}$  for 24 h. The melts were shaken every 6 h to ensure the homogeneity of the molten. Finally, the molten was quenched in ice as previously reported [22]. Five samples of Pb–In alloys with different In content (0.5–15 wt%) were prepared in the same procedures with the composition as shown in Table 1. For the alloys, the percentage of Pb and In was found in accordance with the percentage of mixing Pb and In. The microstructure and composition of the studied alloys were

**Table 1** Chemical composition (weight percent) of the alloys

Alloy nos.	I	II	III	IV	V
Composition	Pb <sub>99.5</sub> In <sub>0.5</sub>	Pb <sub>99</sub> In <sub>1.0</sub>	Pb <sub>95</sub> In <sub>5.0</sub>	Pb <sub>90</sub> In <sub>10</sub>	Pb <sub>85</sub> In <sub>15</sub>

investigated using X-ray diffraction and SEM micrographs. It was found that solid solution phase is formed with homogeneous composition [5].

Phytic acid was obtained from Aldrich and used without further purification at concentration range of  $1 \times 10^{-5}$  to  $1 \times 10^{-3} \text{ M}$ . The structure of phytic acid is shown in Fig. S1 (supporting data). The corrosive solution (1.0 M HCl) was prepared by dilution of AR grade HCl with bidistilled water.

### Electrochemical measurements

The electrochemical measurements were carried out on a planar disk electrode embedded in an Araldite holder. Before each experiment, the surfaces of each working electrode were polished using polishing cloth (polishing machine, Buehler, Lake Bluff, Illinois, USA), until each surface became smooth and mirror like bright, then degreased in pure ethanol and washed in running bidistilled water before being inserted in the polarization cell. The reference electrode was a saturated calomel electrode (SCE) to which all potentials are referred. The cell description was given elsewhere [23]. To remove any surface contamination and air-formed oxide, the working electrode was kept at  $-1.5 \text{ V}$  (SCE) for 5 min in the tested solution. Then it was disconnected, shaken free of adsorbed hydrogen bubbles. To obtain steady-state open circuit potential ( $E_{\text{corr}}$ ) the electrodes were immersed in tested solution for 50 min before starting the measurements. Potentiostat/Galvanostat (EG&G Model 273) was used for the potentiodynamic polarization measurements. The extrapolation of cathodic and anodic Tafel lines was carried out in a potential range of  $-0.20 \text{ V}$  of cathodic and  $+0.1 \text{ V}$  for anodic polarization to avoid the formation of oxide film on the surface with respect to  $E_{\text{corr}}$  at scan rate of  $1 \text{ mV s}^{-1}$  using software version 342C supplied from EG&G Princeton Applied Research. Electrochemical impedance spectroscopy (EIS) measurements were performed with Model VerstStat4-100 Potentiostat/Galvanostat. The frequency range was set from  $10 \times 10^3$  to  $0.01 \text{ Hz}$  with potential amplitude of  $10 \text{ mV}$  at  $E_{\text{corr}}$ . The empirical EIS results were fitted to appropriate equivalent circuit using ZView Software. The morphology of the corrosion products formed on the surfaces of the electrodes was examined using energy-dispersive X-ray spectroscopy analysis (EDX) conducted with scanning electron microscope (SEM), JEOL, Model 5300) with a 3.0-kV operating voltage. The Pb, alloy I and alloy V were immersed in an aqueous solution of HCl



(1.0 M) for 48 h in the absence and presence of  $1 \times 10^{-5}$  M and  $1 \times 10^{-3}$  M of phytic acid at 25 °C.

## Evaluation methods of corrosion parameters

Corrosion current density ( $I_{\text{corr}}$ ) of the investigated electrodes was determined by the extrapolation of cathodic and anodic Tafel lines to  $E_{\text{corr}}$  according to El-Sayed et al. [24]. Each experiment was performed with freshly prepared solution and clean set of electrodes. Measurements were conducted at 25, 35, 45 and 55 °C for each investigated electrode. For this purpose ultrathermostat model Frigther 6000 382 (SELECTA) was used. The inhibition efficiency expressed as inhibition percent ( $\eta$  %) is defined as follows [10]:

$$\eta\% = \frac{I_{\text{uninh.}} - I_{\text{inh.}}}{I_{\text{uninh.}}} \times 100, \quad (1)$$

where  $I_{\text{uninh}}$  and  $I_{\text{inh}}$  are the uninhibited and inhibited corrosion current. The uninhibited corrosion currents were determined in pure (inhibitor free) 1.0 M HCl solution. The inhibited corrosion currents are those determined in the presence of the studied inhibitor at the same temperature.

## Results and discussion

### The corrosion and corrosion inhibition performance of Pb and Pb–In alloys

The results of  $E_{\text{corr}}$  for Pb and Pb–In alloys (Fig. 1a) indicate that  $E_{\text{corr}}$  shifts to more negative direction in the case of alloy I (0.5% In) compared with that value of pure Pb. This negative shift is associated with the pronounced decrease in the corrosion rate of alloy I compared with that of pure Pb in the absence of the PA inhibitor (Fig. 1b). However,  $E_{\text{corr}}$  shifts to positive direction at higher indium contents (alloys II and III), and this positive shift is associated with relative increase in the corrosion rate (Fig. 1b) up to 5% In compared with that of alloy I [9]. This indicates that the presence of indium as a minor alloying element (0.5%) reduces the corrosion rate, i.e. decreases the density of active sites on the alloy surface compared with that of Pb [25]. However, the relative increase in corrosion rate with increasing In content in the alloy up to 5% can be attributed to the lower hydrogen over-potential of the mentioned alloys compared with that of alloy I. This behavior can be ascribed to the change in the amount of solid solution phase on the surface, with increasing In content, leading to depolarizing action of the formed particles. The negative shift in  $E_{\text{corr}}$  (Fig. 1a) of the alloys IV and V (higher In content) relative to that observed of pure Pb (Fig. 1a), with a decrease in the corrosion rate, can

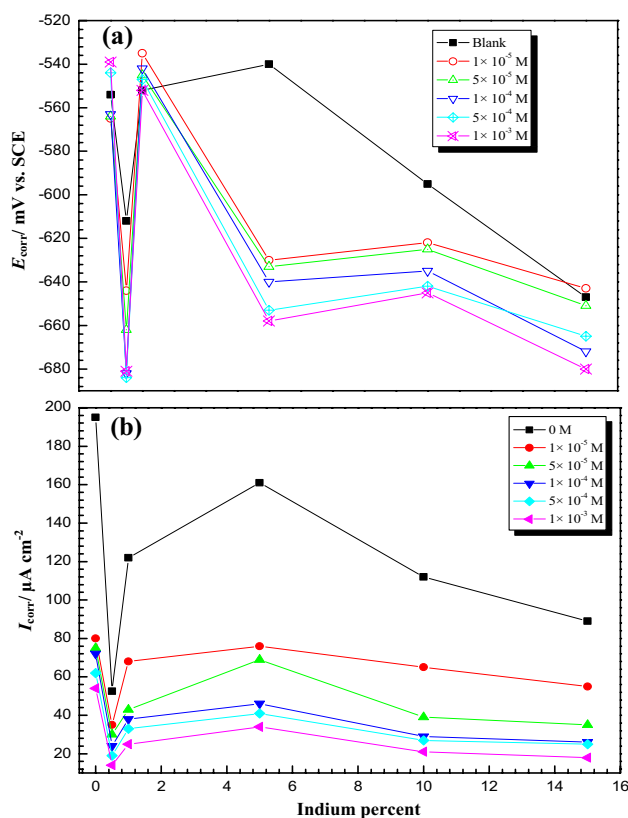


**Fig. 1** Comparison between **a** corrosion potential,  $E_{\text{corr}}$  and **b** corrosion current density,  $I_{\text{corr}}$  of Pb and Pb–In alloys in 1 M solution of HCl containing various concentrations of PA inhibitor at 25 °C after 50 min of exposure

be attributed to the much higher formation of solid solution phase, leading to the increase of the cathodic to anodic area ratio. This fact can be due to the higher formation of solid solution phase on the alloy surface leading to less heterogeneous surface.

Potential-time curve for Pb (line 1 and 2) and alloy V (line 3 and 4) in 1.0 M HCl solution in the absence and presence of 1 mM of PA at 25 °C is shown in Fig. S2 (supporting data). It is clear from the curve that the corrosion potential ( $E_{\text{corr}}$ ) of Pb and alloy V electrodes in the studied medium is shifted to more noble direction until steady-state potential is determined. Addition of PA inhibitor molecule to the HCl solution produces a positive shift in  $E_{\text{corr}}$ , i.e.; the potential was shifted to more noble direction. This behavior due to the PA inhibitor molecules reduces the active site on the electrode surface by the adsorption on these active sites.

Corrosion parameters were calculated based on the cathodic and anodic potential versus current density characteristics in the Tafel potential region [26, 27]. Figure 2a, b represents the experimental results from the polarization curves without and with the addition of different concentrations of phytic acid in the case of alloys I and V (0.5%

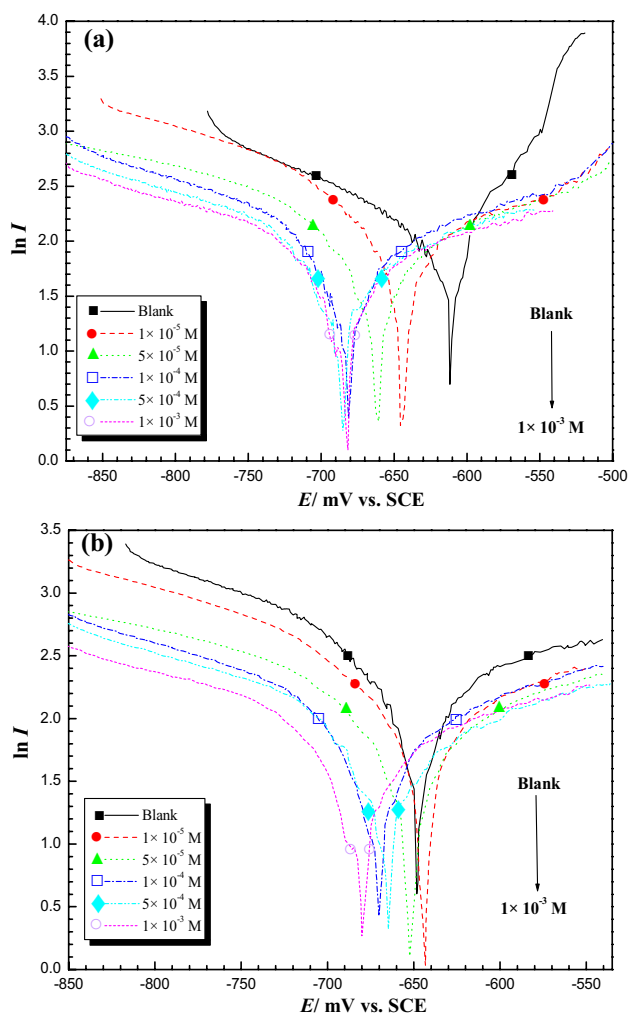


**Fig. 2** Polarization curves for **a** alloy I (Pb–0.5In) and **b** alloy V (Pb–15In) in 1 M HCl in the absence and presence of various concentrations of Phytic acid inhibitor at 25 °C

and 15% In). The values of  $I_{\text{corr}}$  for the studied metal and its alloys without and with the inhibitor, respectively, were determined by the extrapolation of the cathodic and anodic Tafel lines to the  $E_{\text{corr}}$ . It can be seen that the presence of phytic acid results in a marked shift in both cathodic and anodic branches of the polarization curves towards lower current densities. As the inhibitor concentration increases the corrosion current is considerably decreased. A slight negative shift in the  $E_{\text{corr}}$  in the presence of lower concentrations ( $1 \times 10^{-5}$ – $1 \times 10^{-4}$  M), while positive shift at higher concentrations ( $5 \times 10^{-4}$ – $10^{-3}$  M), is observed in the case of Pb (Table 2), indicating that the active sites on the electrode surface are blocked by inhibitor molecules. However,  $E_{\text{corr}}$  shifts to more negative direction with increasing the concentration in the case of the investigated alloys. This trend can be ascribed to the changes in potential of hydrogen evolution reaction towards more negative values, with increasing

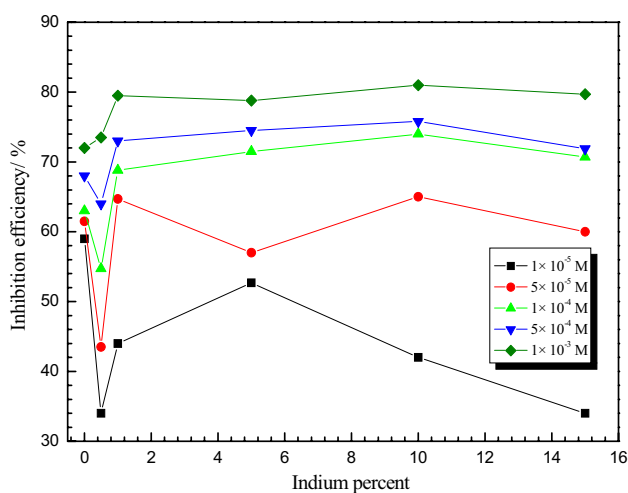
inhibitor concentrations. That shift may indicate blocking of active cathodic sites. This opposite effect at higher concentrations of the inhibitor in the case of alloys compared with that of pure Pb can be ascribed to the presence of Pb–In phase on the alloy surface.

Table 2 represents the influence of the inhibitor concentration on the corrosion parameters of Pb, alloys I and V (as examples of the investigated alloys) in 1 M HCl solution. The data show that  $I_{\text{corr}}$  decreases with increasing concentration of the inhibitor. This indicates the inhibiting action of phytic acid on the corrosion of pure Pb and its investigated alloys. The cathodic Tafel slope ( $\beta_c$ ) in Table 2 is significantly increased, while the anodic Tafel slope ( $\beta_a$ ) decreased in the inhibited solution compared with the corresponding values for uninhibited solution. The pronounced increase in the inhibited  $\beta_c$  value reveals the effect of inhibitor to reduce the surface area available for hydrogen evolution reaction. In addition to the above assertion, it can be noted that the displacement of the  $E_{\text{corr}}$  value obtained in the solution with the addition of PA is not greater than 85 mV compared to the bare HCl solution indicating that the PA is mixed-type inhibitor, i.e., it would affect both the electrochemical hydrogen evolution reaction and the anodic dissolution of Pb and Pb–In alloys [28]. It is found that the inhibition efficiency ( $\eta$  %) increases as a result of an increase in the concentration of the inhibitor. These results suggest that retardation of the electrode processes occurs, at both cathodic and anodic sites, as a result of the coverage of these sites by the inhibitor molecules. In other words, the reduction of either the anodic and cathodic reaction or both arises from the adsorption of the inhibitor on the corresponding active sites.

The data in Figs. 1b and 3 represent the corrosion parameters of Pb and its investigated alloys in the absence and presence of phytic acid at 25 °C. It is observed that the  $I_{\text{corr}}$  decreases and inhibition efficiency ( $\eta$  %) increases of the investigated electrodes with increasing the concentration of phytic acid. The results exhibited that  $\eta$  % of the studied inhibitor in the case of alloy I (0.5% In) is lower than that of the corresponding value obtained for Pb and other investigated alloys (II–V) at all studied concentrations (except at  $1 \times 10^{-3}$  M). This behavior may be attributed to the less adsorption of inhibitor molecules on the alloy surface to block the active sites. It is assumed that the presence of indium as a minor alloying element decreases the active sites density at the surface [29]. Therefore, lower adsorbability of the inhibitor molecules occurs. However, the values of  $\eta$  % for alloy I and Pb at higher concentration ( $10^{-3}$  M) are approximately equal ( $\approx 73\%$ ). But, it is observed that  $\eta$  % values of alloys II and III (1 and 5% In) are higher than that of alloy I, particularly at lower concentrations ( $10^{-5}$  M). This behavior can be interpreted on the basis that the presence of In content in the alloy more than 0.5% (at 1–5%) increases the active sites on the surface compared with those of alloy

**Table 2** Corrosion parameters for pure Pb, alloy I and alloy V in 1.0 M HCl solution containing various concentrations of PA inhibitor at 25 °C after 50 min of exposure

Metal and alloys	Conc. of inhibitor (mol/L)	$I_{\text{corr}}$ ( $\mu\text{A cm}^{-2}$ )	$-E_{\text{corr}}$ (mV) (SCE)	$\beta_a$ (mV $\text{dec}^{-1}$ )	$-\beta_c$ (mV $\text{dec}^{-1}$ )	$\theta$	$\eta$ %
Pb	Blank	195	554	41	138	–	–
	$1 \times 10^{-5}$	80	565	37	233	0.59	59
	$5 \times 10^{-5}$	75	564	35	235	0.61	61.5
	$1 \times 10^{-4}$	72	563	33	210	0.63	63
	$5 \times 10^{-4}$	62	544	29	209	0.68	68
	$1 \times 10^{-3}$	54	539	28	206	0.72	72
Alloy I	Blank	52.5	612	42	149	–	–
	$1 \times 10^{-5}$	35	644	34	230	0.34	34
	$5 \times 10^{-5}$	30	662	31	228	0.43	43.5
	$1 \times 10^{-4}$	24	682	29	222	0.54	54.7
	$5 \times 10^{-4}$	19	684	27	218	0.64	64
	$1 \times 10^{-3}$	14	681	21	214	0.73	73.5
Alloy V	Blank	89	647	49	149	–	–
	$1 \times 10^{-5}$	55	643	32	220	0.34	34
	$5 \times 10^{-5}$	35	651	32	220	0.60	60
	$1 \times 10^{-4}$	26	672	29	215	0.70	70.7
	$5 \times 10^{-4}$	25	665	25	211	0.72	71.9
	$1 \times 10^{-3}$	18	680	21	209	0.79	79.7

**Fig. 3** Comparison between inhibition efficiency of Pb and its alloys in 1 M solution of HCl containing various concentrations of phytic acid at 25 °C

I. This behavior can be supported with the higher corrosion of current density of the two mentioned alloys in pure acid solution compared with that of alloy I (see Table 2). On the other hand, relative decrease in  $\eta$  % value is observed at higher In content (10 and 15%) compared with that of alloys II and III at lower inhibitor concentration ( $10^{-5}$  M). This behavior can be attributed to less active site on the surface, leading to less adsorbability of the inhibitor molecules. This fact would be due to the higher formation of

solid solution phase in the alloy, having the effect to decrease the heterogeneity on the surface. However, it is interesting to observe that the inhibition efficiency values seem to almost be equal for some investigated alloys (II to V) at higher concentrations. This behavior can be ascribed to that the most electrode surface of the investigated alloys was covered by adsorbed inhibitor molecules. Consequently, the majority of active sites are blocked. In other words, the increase of inhibition efficiency with increasing the concentration of the inhibitor is due to the increase of the adsorption amount and the coverage of inhibitor molecules.

It is well known that the sign of  $\Phi$  potential value defines the type of charge on the surface. According to Antropov [30, 31] the potential of zero charge of Pb in acidic media is negatively charged ( $E_{q=0}$  is equal to  $-0.56$  V). The value of  $\Phi$  potential was calculated according to the following equation:

$$\Phi = E_{\text{corr}} - E_{q=0} \quad (2)$$

Hence, the value of  $\Phi$  potential of Pb is  $+0.25$  V. This indicates that the surface of Pb is positively charged at  $E_{\text{corr}}$ . According to El-Sayed [32], when the corrosive medium contains adsorbable anions, such as  $\text{Cl}^-$  ions, they are first adsorbed on the electrode surface by creating oriented dipoles. Consequently, the surface of the investigated electrodes becomes negatively charged. The distribution of charge densities in the phytic acid molecule was calculated by  $\text{PM}_3$  semi-empirical methods using Win MOPAC 2.71 software. The structure of the phytic acid is given in Fig. S1.

The electron density on phytic acid groups reveals that the largest partial negative charges ( $\delta^-$ ) are localized at numbers 1 and 2 of OH groups. Accordingly, the acidity of phytic acid exists in aqueous solution as protonated cationic species through OH<sup>-</sup> groups (OH<sub>2</sub><sup>+</sup>). Therefore, it may be assumed that phytic acid adsorption can also occur via electrostatic interaction between a negatively charged surface and the partial positive charge of protonated oxygen atoms. Consequently, the adsorption of the inhibitor molecule on the surface can be suggested as shown in Fig. 4.

When we compared our study with the literature data, Dus and Smialovska studied the inhibition effect of diethyl selenophosphates on Pb electrode in acidic media [13]. They found that the inhibition efficiency in the presence of 0.4 mmol/L of inhibitor was found to be 41%. Vani et al. [33] also investigated the inhibition performance of polyethylene glycol (PEG) on Pb and Pb free solders in 1.0 N HCl containing 20 ppm of PEG using weight loss and potentiodynamic polarization measurements. They showed that the inhibition efficiency of this inhibitor was around 66%. In another study, Helal et al. [11] investigated the inhibition efficiencies of some amino acids, namely glycine, alanine, valine, and histidine on Pb in aqueous solutions with different pHs (2, 7 and 12). They found that the inhibition efficiencies were around 37.2, 70.4, 45.96 and 35.7%, respectively. Moreover, the effect of a new series of organic amines as suppressants of Pb corrosion in 0.3 M HCl solution was studied by Badawy et al. [12]. The used inhibitors were pyrazole derivatives, such as 3(5) amino, 5(3) phenyl pyrazole (PP), 3(5) amino, 5(3)[4-methyl phenyl] pyrazole (MePP), 3(5) amino, 5(3)[4-methoxy phenyl] pyrazole (MeOPP) and 3(5) amino, 5(3)[4-chloro phenyl] pyrazole (CIPP). At the same concentration, the inhibition efficiency increases in

the following order: MeOPP (20%) < CIPP (36.52) < PP (58.26%) < MePP (70%). Our potentiodynamic polarization and EIS measurements support the literature data taking into account the physical and chemical meaning of the inhibition characteristics of phytic acid compound.

### Effect of temperature

In order to get more information about the type of adsorption and the effectiveness of the studied inhibitor, potentiodynamic polarization measurements were performed at different temperatures (25–55 °C) for Pb and alloy I (as representative alloy) in 1 M HCl solution without and with selected concentrations of phytic acid. The corrosion parameters showed that increasing of the solution temperature leads to an increase in the  $I_{\text{corr}}$ , and  $E_{\text{corr}}$  shifts to more positive direction. These results reflect the enhancement of the cathodic hydrogen evolution reaction as well as anodic dissolution of Pb and its alloys with the increase of temperature [34, 35]. Similar results were obtained by Hassan [36] for corrosion inhibition of mild steel by triazole derivatives in HCl solution. Therefore, the increase of corrosion is pronounced with increasing temperature [37]. On the other hand, the slopes of  $\beta_c$  and  $\beta_a$  Tafel lines remain almost unchanged with increasing temperature. This indicates that the temperature only activates the surface for corrosion without affecting the mechanism.

The data exhibited that the inhibition efficiency decreases with increasing temperature of Pb and its studied alloy. Figure 5a, b represents the relation between the inhibition efficiency ( $\eta$  %) and the concentration of phytic acid for Pb and alloy I (0.5% In) at different temperatures. This behavior would be due to the decrease in the strength of

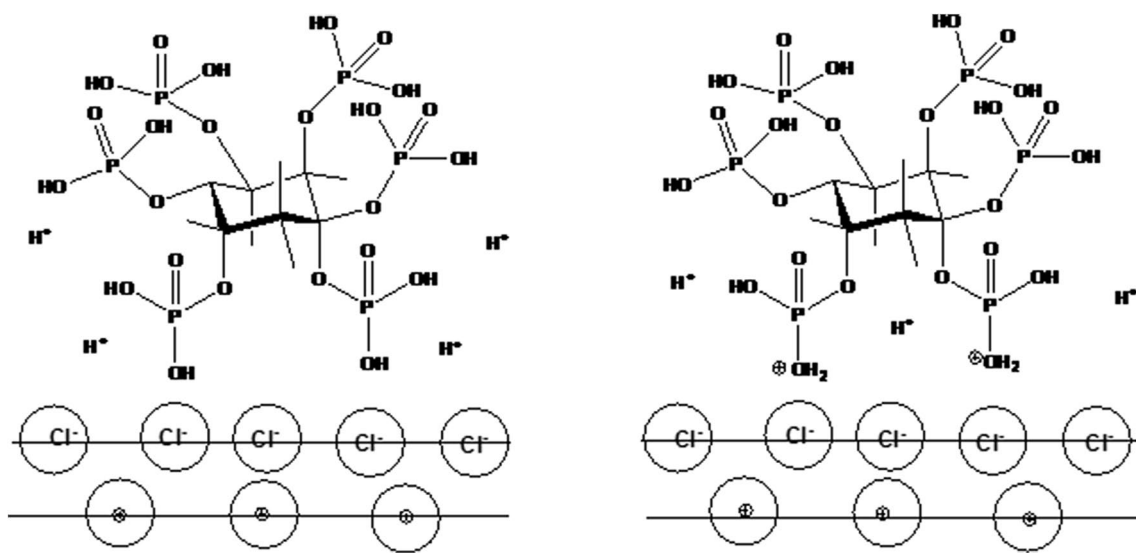
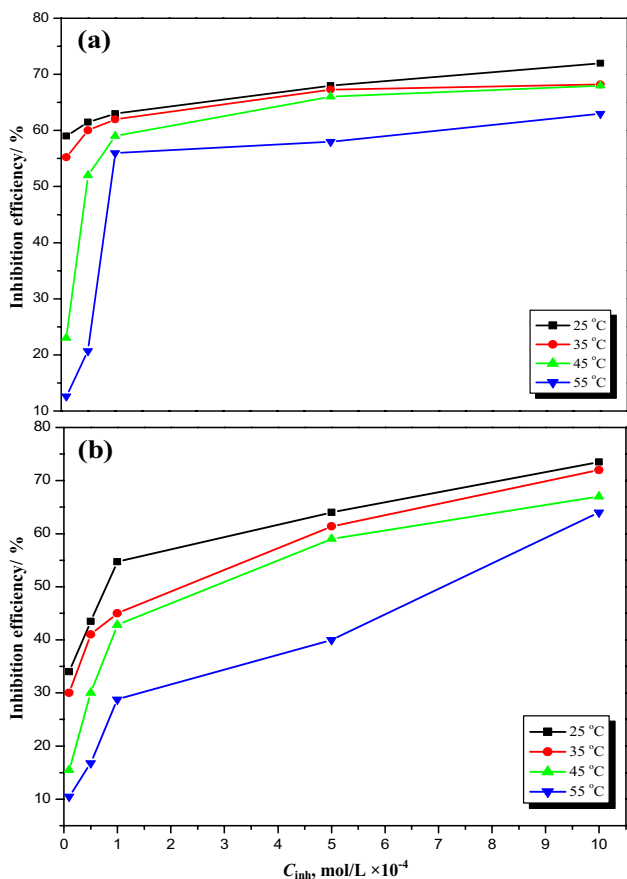


Fig. 4 Mode of adsorption of phytic acid on the metal and/or alloy surface





**Fig. 5** Effect of various concentrations of PA on the inhibition efficiency for **a** pure Pb and **b** alloy I in 1 M HCl at different temperatures

the adsorption process at higher temperatures, suggesting that the physical adsorption is the type of adsorption of the inhibitor molecules on the surface. The adsorption of the inhibitor on the electrode surface leads to the formation of a physical barrier that reduces the metal reactivity in the electrochemical reactions.

Arrhenius plots for Pb and Pb–0.5In alloy in the absence and presence of the investigated inhibitor in 1.0 M solution of HCl are shown in Fig. 6. The activation energy can be expressed by the Arrhenius equation [10] as follows:

$$\log I_{\text{corr}} = \log A - \frac{E_a}{2.33R} \frac{1}{T}, \tag{3}$$

where  $I_{\text{corr}}$  is the corrosion current density,  $A$  is an Arrhenius pre-exponential factor,  $E_a$  is the apparent activation energy of the corrosion process,  $T$  is the absolute temperature and  $R$  is the universal gas constant [38]. Some relevant information about the adsorption mechanism of the inhibitor can be obtained by comparing  $E_a$  values in both the absence and presence of the corrosion inhibitor. The values of the apparent activation energy ( $E_a$ ) of Pb and Pb–0.5In alloy for

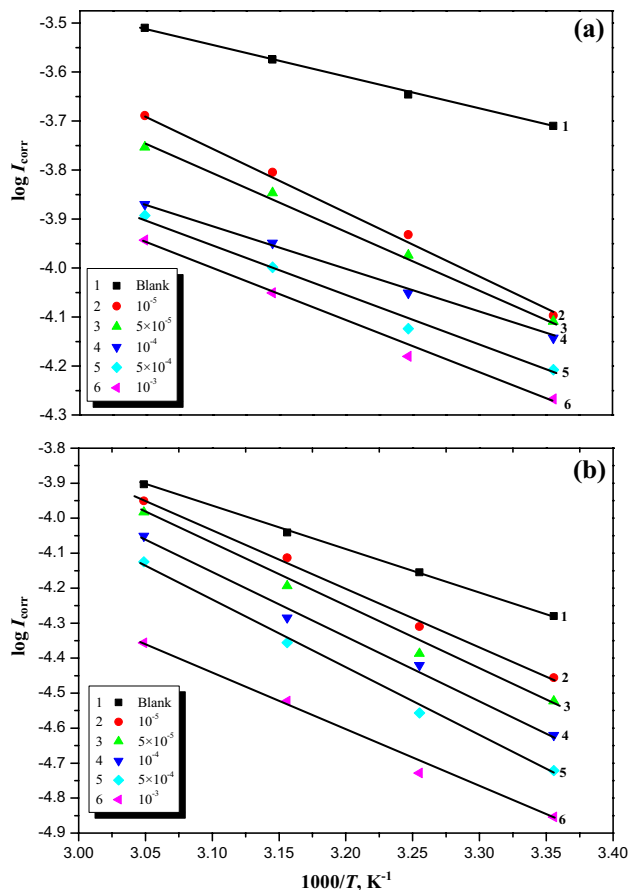


**Fig. 6** Arrhenius plots for **a** Pb and **b** alloy I corrosion in 1 M HCl containing various concentrations of phytic acid

corrosion determined from the slope of  $\log I_{\text{corr}}$  versus  $1/T$  plots are given in Table 3. It is observed that the  $E_a$  values for Pb and Pb–0.5In alloy in 1 M HCl in the presence of PA

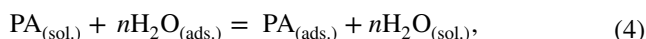
**Table 3** Apparent activation energy in kJ/mol for Pb and Pb–0.5In alloy in 1.0 M HCl solution containing various concentrations of PA inhibitor

Metal and alloy	Concentration (mol/L)	$E_a$ (kJ/mol)
Pure Pb	0.0	16.69
	$1 \times 10^{-5}$	21.43
	$5 \times 10^{-5}$	24.02
	$1 \times 10^{-4}$	24.84
	$5 \times 10^{-4}$	26.51
	$1 \times 10^{-3}$	27.80
Pb–0.5In alloy	0.0	23.63
	$1 \times 10^{-5}$	32.48
	$5 \times 10^{-5}$	34.45
	$1 \times 10^{-4}$	35.04
	$5 \times 10^{-4}$	36.54
	$1 \times 10^{-3}$	37.81

inhibitor increase with increasing the inhibitor concentration. The data show that the values of  $E_a$  of the two investigated electrodes in HCl solution in the presence of PA are higher than those in the uninhibited acid solution. Thus the presence of inhibitor enhances the activation energy barrier of the corrosion of the tested electrodes, whereby reducing the corrosion rate. The higher values of activation energy ( $E_a$ ) indicate that the strong physical adsorption of the phytic acid makes the dissolution of Pb or its alloy in the acid solution more difficult [4]. One can conclude that the increase in activation energy with increasing additive concentration, in addition to the decrease in  $\eta$  % in the presence of inhibitor with temperature, is suggestive of physisorption of the inhibitor molecule on the surface of Pb and Pb–0.5In alloy.

### Adsorption isotherm and thermodynamic parameters for the corrosion process

Adsorption isotherms are very important in determining the mechanism of organo-electro chemical reactions. The degree of surface coverage ( $\theta$ ) for different concentrations of the compound can be evaluated from potentiodynamic polarization measurements [39]. The determination of the type of adsorption isotherm itself provides information on the adsorption process such as surface coverage, adsorption equilibrium constant and information on the interaction between the organic compound and electrode surface. During corrosion inhibition of metals and alloys, the nature of the inhibitor on the corroding surface has been deduced in terms of adsorption characteristics of the inhibitor. Furthermore, the solvent ( $H_2O$ ) molecules could also be adsorbed at metal–solution interface. So the adsorption of the inhibitor molecules from the aqueous solution can be regarded as a quasi-substitution process between the organic compounds in the aqueous phase [ $PA_{(sol.)}$ ] and water molecules at the electrode surface [ $H_2O_{(ads.)}$ ] [40]:



where  $n$  is the size ratio, that is, the number of water molecules replaced by one PA inhibitor molecule. Basic information on the interaction between the inhibitor and the electrode surface can be provided by the adsorption isotherm. In order to obtain the isotherm, the linear relation between the degree of surface coverage ( $\theta$ ) obtained from Tafel polarization ( $\theta = \eta \% / 100$ ) and inhibitor concentration ( $C_{inh.}$ ) must be found. Attempts were made to fit the  $\theta$  values to the various isotherms including Langmuir, Temkin, Frumkin and Flory–Huggins. The best fit was obtained by Langmuir isotherm. This isotherm is based on the assumption that all adsorption sites are equivalent and that particle binding occurs independently from nearby sites, whether occupied or not [41]. According to this isotherm,  $\theta$  is related to  $C$  by

$$\frac{C_{inh}}{\theta} = C_{inh} + \frac{1}{K_{ads}} \quad (5)$$

$$K_{ads} = \frac{1}{55.5} \exp\left(-\frac{\Delta G_{ads}^0}{RT}\right) \quad (6)$$

where  $K_{ads}$  is the equilibrium constant of the inhibitor adsorption process and  $C_{inh}$  is the inhibitor concentration. Straight lines of  $C_i/\theta$  versus  $C_i$  plots indicate that the adsorption of the inhibitor molecule on the electrode surface obeyed Langmuir adsorption model (Fig. 7). The regression coefficients of the fitted curves are around unity ( $R^2 > 0.9892$ , Table 4), which signifies that the adsorption of PA molecules on Pb and its alloys obeys the Langmuir adsorption model. The inhibition tendency of the tested inhibitor is due to the adsorption of this molecule on the electrode surface [42].  $K_{ads}$  values were calculated from the intercepts of the straight lines on the  $C_i/\theta$  axis [43] and correlated to the standard free energy of adsorption ( $\Delta G_{ads}^0$ ) using the following equation [44]:

The value 55.5 in the above equation was the molar concentration of water in solution in mol/L [45]. The relatively high value of the adsorption equilibrium constant ( $K_{ads}$ ; Table 4) reflects the high adsorption ability of this inhibitor on the electrode surface [46]. It is also noted that the high value of  $K_{ads}$  for pure Pb indicates stronger adsorption on the metal surface than that on the other alloys. Large values of  $K_{ads}$  imply more efficient adsorption and hence better inhibition efficiency [47]. It is seen that the values of  $K_{ads}$  are decreased with an increase in temperature, confirming the suggestion that the investigated inhibitor is physically adsorbed on the surfaces of Pb and Pb–In alloys, and the strength of the adsorption decreases with temperature.

Generally, the values of  $\Delta G_{ads}^0$  up to  $-20$  kJ mol $^{-1}$  are consistent with physisorption, while those around  $-40$  kJ mol $^{-1}$  or higher are associated with chemisorption as a result of the sharing or transfer of electrons from organic molecules to the metal surface to form a coordinate bond [48]. In the present study, the values of  $\Delta G_{ads}^0$  obtained for the studied PA inhibitor on pure Pb and Pb–In alloys in 1.0 M HCl solution range between  $-25.50$  and  $-26.06$  kJ mol $^{-1}$  (Table 4). These results indicate that the adsorption mechanism of the investigated inhibitor on these electrodes involves both mechanisms, chemical and physical adsorption. Physical adsorption is due to the electrostatic attraction between the ions or dipoles of the inhibiting species and the electrically charged surface of the electrode. Thermodynamically,  $\Delta G_{ads}^0$  is related to the enthalpy ( $\Delta H_{ads}^0$ ) and entropy ( $\Delta S_{ads}^0$ ) of adsorption process,  $\Delta H_{ads}^0$  and  $\Delta S_{ads}^0$ , respectively, by equation [49]:

$$\Delta G_{ads}^0 = \Delta H_{ads}^0 - T\Delta S_{ads}^0 \quad (7)$$

Figure 8 shows the plot of  $\Delta G_{ads}^0$  versus  $T$  which gives a straight line with an intercept of  $\Delta H_{ads}^0$  and a slope of  $-\Delta S_{ads}^0$  [49]. The value of  $\Delta H_{ads}^0$  can provide important





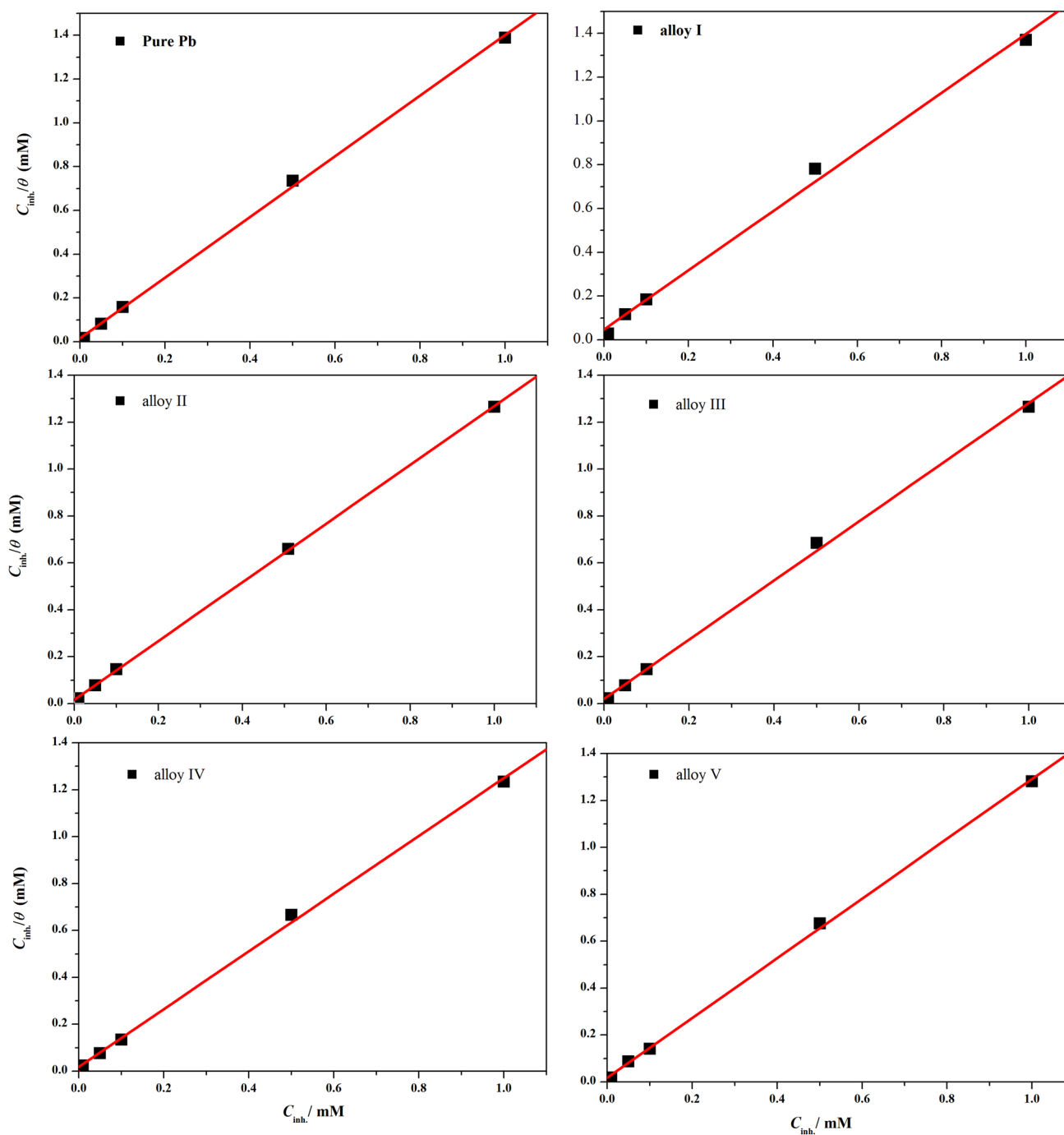


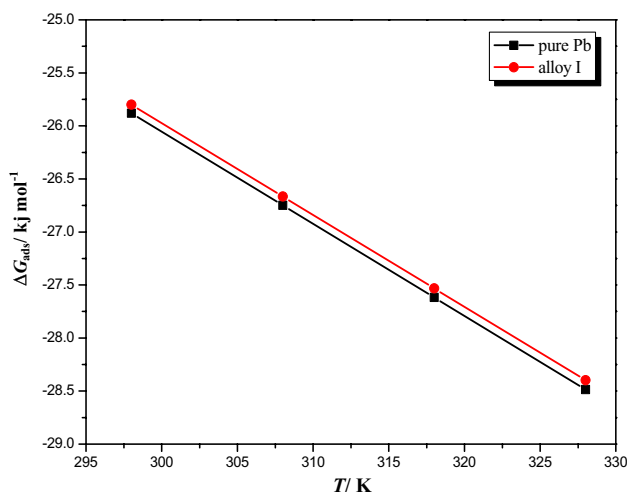
**Fig. 7** Langmuir adsorption model ( $C_i/\theta$  vs.  $C_i$ ) fitting of the data obtained from Tafel polarization measurements for Pb and Pb–In alloys in 1 M HCl solution containing different concentrations of phytic acid at 25 °C

information about the adsorption mechanism of an inhibitor. For an exothermic adsorption process,  $\Delta H_{\text{ads}}^0 < 40 \text{ kJ mol}^{-1}$  reflects physisorption, whereas  $\Delta H_{\text{ads}}^0$  value approaching  $100 \text{ kJ mol}^{-1}$  points to chemical adsorption [49]. In our case, the calculated value of  $\Delta H_{\text{ads}}^0$  for Pb and alloy I in HCl solution containing various concentrations of PA inhibitor was  $-25.26$  and  $-25.55 \text{ kJ mol}^{-1}$ , respectively. Based

on this result, the adsorption process was exothermic and the mechanism of adsorption was physisorption which is in good agreement with the variation of inhibition efficiency with temperature (Fig. 5). The  $\Delta S_{\text{ads}}^0$  values were found  $+86.91$  and  $+86.58 \text{ kJ/mol}$  for Pb and alloy I, respectively. The negative value of  $\Delta H_{\text{ads}}^0$  indicates that the adsorption of inhibitor molecule is an exothermic process [50]. The

**Table 4** Thermodynamic parameters for the adsorption of the studied inhibitor on Pb and Pb–In alloys in 1.0 M HCl solution at 25 °C

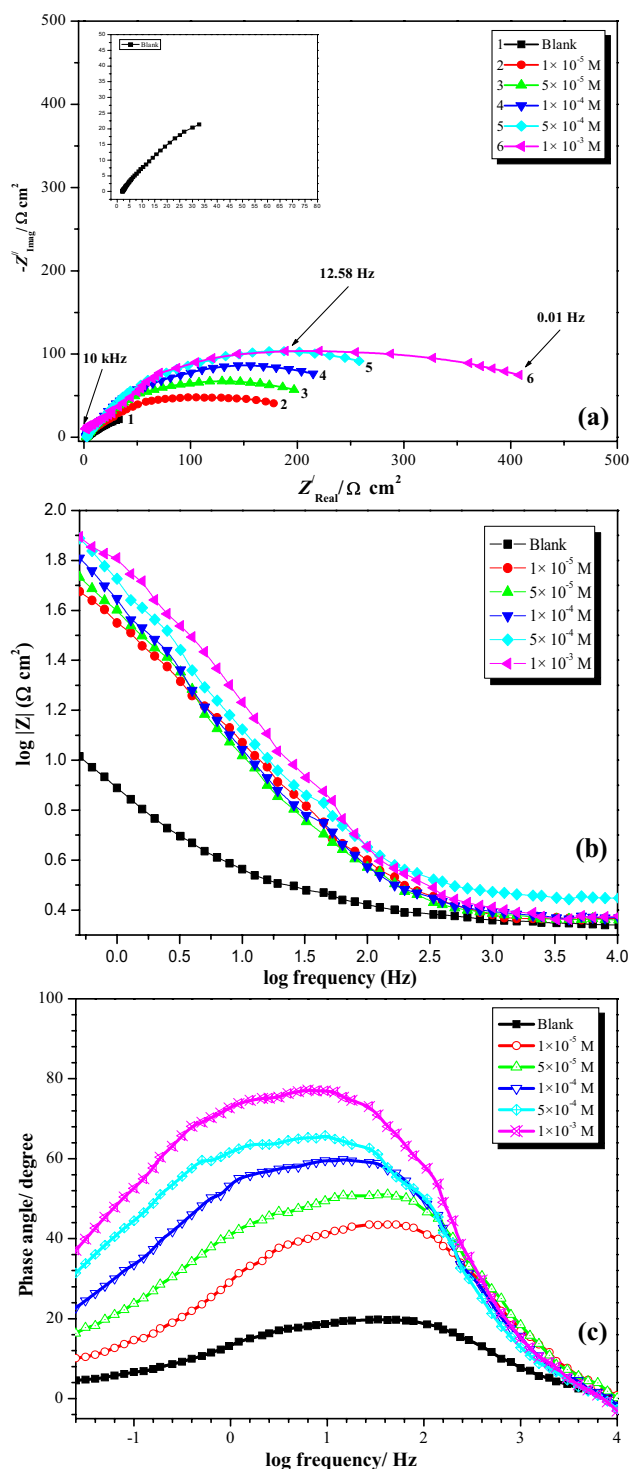
Metal and alloys	Slope	Regression coefficients, $R^2$	$K_{\text{ads}}, M^{-1}$	$\Delta G_{\text{ads}}^0$ (kJ mol $^{-1}$ )
Pb	1.05	0.9976	625	−25.88
Alloy I	1.07	0.9897	606	−25.80
Alloy II	1.09	0.9993	611	−25.82
Alloy III	1.10	0.9892	537	−25.50
Alloy IV	1.12	0.9973	671	−26.06
Alloy V	1.08	0.9898	645	−25.96

**Fig. 8** Variation of  $\Delta G_{\text{ads}}^0$  versus  $T$  of pure Pb and alloy I in 1.0 M HCl solution containing  $1 \times 10^{-3}$  M phytic acid

positive  $\Delta S_{\text{ads}}^0$  value could be linked to rise in solvent energy and higher water desorption entropy [51].

### Electrochemical impedance measurements (EIS)

It is well known that EIS is a powerful technique for studying corrosion mechanisms and adsorption phenomena [52]. In order to support the data obtained from the potentiodynamic polarization, EIS of Pb and its investigated alloys in 1 M HCl containing various concentrations of phytic acid (PA) was examined. The complex plane of impedance at  $E_{\text{corr}}$  was plotted as shown in Figs. 9 and 10. The impedance spectra recorded for pure Pb and its investigated alloys (except alloy III) in the absence and presence of various concentrations of the inhibitor display one capacitive loop. The shape of spectra, which composed of one semicircle, represents the presence of corrosion reaction at the surface/electrolyte interface. It can be concluded from these plots (Figs. 9 and 10) that the

**Fig. 9** Nyquist (a), bode modulus (b) and bode phase angle plots (c) for Pb in 1 M HCl containing various concentrations of phytic acid inhibitor, measured at  $E_{\text{corr}}$  and at 25 °C

impedance response of Pb and its alloy has significantly changed after the addition of phytic acid in various concentrations to corrosive solution. This can be attributed to the increase of the substrate impedance with increasing the

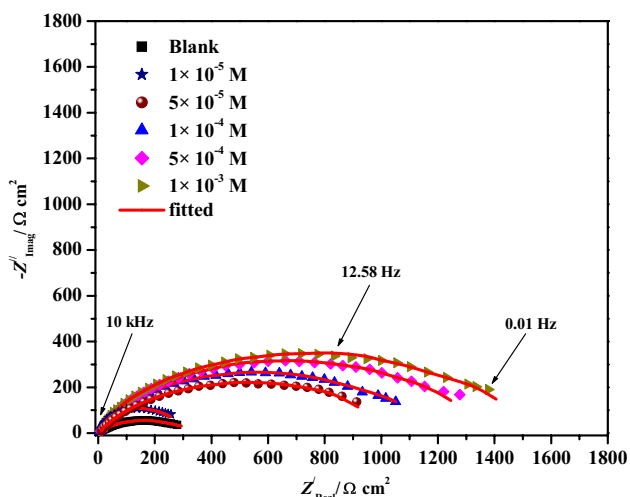


**Fig. 10** Nyquist plot for alloy I in 1 M HCl containing various concentrations of phytic acid inhibitor, measured at  $E_{corr}$  and at 25 °C

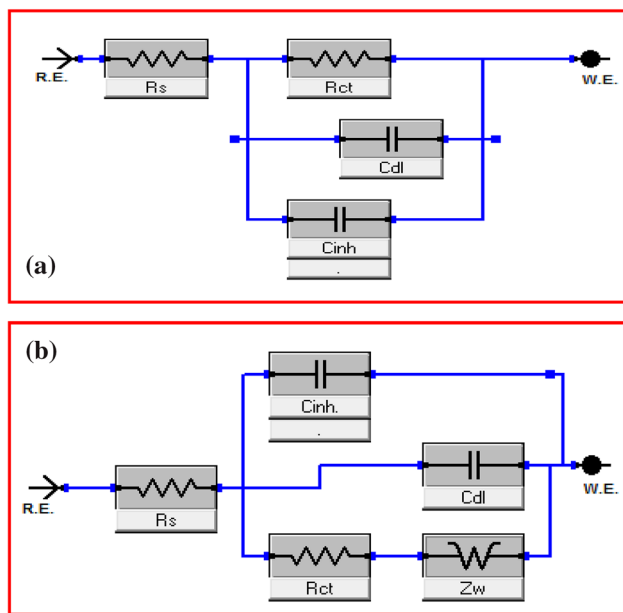


**Fig. 11** Equivalent circuit model used in the fitting of impedance data of **a** semicircle without Warburg tail and **b** semicircle with Warburg tail

inhibitor concentration. The semicircle seems to deviate from the ideal capacitive behavior is due to the surface heterogeneities, roughness factors and adsorption of  $Cl^-$  ions [53–55]. However, the semicircle is gradually improved as the concentration of phytic acid is increased. As can be seen from the data in Figs. 9 and 10, the size of the loop in pure HCl is increased with increasing the inhibitor concentration, indicating that the charge transfer is more difficult [4]. The experimental values are correlated to the simple

equivalent circuit model presented in Fig. 11 a. The calculated equivalent circuit parameters for Pb and its alloys (I and V) in the absence and presence of phytic acid are presented in Table 5. Generally, the Bode plots (Fig. 9b) show a single phase maximum at intermediate frequencies, which indicates the presence of one time constant, representing the electrode process. Also, it was found that the phase angles (Fig. 9c) are increased with increasing the concentration of PA close to 90°, indicating eminent inhibitive behavior is due to the formation of the protective layer on the electrode surface by inhibitor molecules [56]. Moreover, this behavior can be explained on the basis that decreasing in the surface heterogeneity is due to adsorption of the inhibitor molecules on the most active sites [57], and consequently retards the adsorption of  $Cl^-$  ions. The charge transfer resistance ( $R_{ct}$ ) and the capacity of the double layer ( $C_{dl}$ ) were calculated according to the fitting of the impedance data to the circuits of Fig. 11. Double layer capacitance  $C_{dl}$  was calculated using the following equation [56]:

$$f(-Z''_{max}) = \frac{1}{2\pi C_{dl} R_{ct}}, \tag{8}$$

where  $-Z''_{max}$  is the maximum imaginary component of the impedance. The inhibition efficiency ( $\eta$  %) was calculated using the following equation [56]:

$$\eta (\%) = \frac{R_{ct} - R_{ct}^0}{R_{ct}^0} \times 100, \tag{9}$$

where  $R_{ct}$  and  $R_{ct}^0$  are the charge transfer resistance values in the inhibited and uninhibited solution, respectively.

The data in Table 5 show that the charge transfer resistance ( $R_{ct}$ ) increases with increasing concentration of the inhibitor, and the inhibiting power is higher. A large charge transfer resistance is associated with a slower corroding system [58]. Furthermore, a better protection provided by an inhibitor is associated with a decrease in capacitance of the metal or its investigated alloys [59]. The decrease in  $C_{dl}$ , which results from a decrease in local dielectric constant and/or an increase in the thickness of the electrical double layer, suggests that the inhibitor molecules act by adsorption on the metal or alloy–solution interface [60].

However, the complex-plane impedance plots of alloy III (5% In) in the absence and presence of the inhibitor exhibit different behavior compared with that of the other alloys. The recorded spectra show one capacitive loop at the higher frequency range (HF) followed by the Warburg Tail at lower frequency (LF) (Fig. 12). The data in Fig. 12 show that the Warburg impedance ( $Z_w$ ) is related to the diffusion of soluble species from the alloy surface to the bulk of solution [61]. The diameter of the capacitive loop ( $R_{ct}$ )

**Table 5** Electrochemical parameters and inhibition efficiencies derived from electrochemical impedance spectroscopy for Pb, alloy I and alloy V in 1.0 M HCl solution containing various concentrations of phytic acid at 25 °C

Metal and alloys	Conc. of inhibitor (mol/L)	$R_s$ ( $\Omega \text{ cm}^2$ )	$R_p$ ( $\Omega \text{ cm}^2$ )	$C_{dl}$ ( $\text{F cm}^{-2} \times 10^{-8}$ )	$\theta$	$\eta$ %
Pb	Blank	2.01	92	105	–	–
	$1 \times 10^{-5}$	1.25	227	7.0	0.59	59.47
	$5 \times 10^{-5}$	1.13	272	5.8	0.66	66.17
	$1 \times 10^{-4}$	0.7	313	5.1	0.70	70.60
	$5 \times 10^{-4}$	0.3	340	4.7	0.72	72.94
	$1 \times 10^{-3}$	0.4	370	4.3	0.75	75.13
Alloy I	Blank	5	365	3.9	–	–
	$1 \times 10^{-5}$	6	509	3.6	0.28	28
	$5 \times 10^{-5}$	5	1112	1.43	0.67	67
	$1 \times 10^{-4}$	1.2	1267	1.25	0.71	71
	$5 \times 10^{-4}$	3	1340	1.18	0.72	72.7
	$1 \times 10^{-3}$	2.5	1412	1.13	0.74	74.1
Alloy V	Blank	4.5	326	4.47	–	–
	$1 \times 10^{-5}$	5.5	424	3.75	0.23	23
	$5 \times 10^{-5}$	1	818	1.94	0.60	60
	$1 \times 10^{-4}$	2.3	1095	1.45	0.70	70
	$5 \times 10^{-4}$	3.4	1129	1.41	0.71	71
	$1 \times 10^{-3}$	2.3	1185	1.34	0.72	72

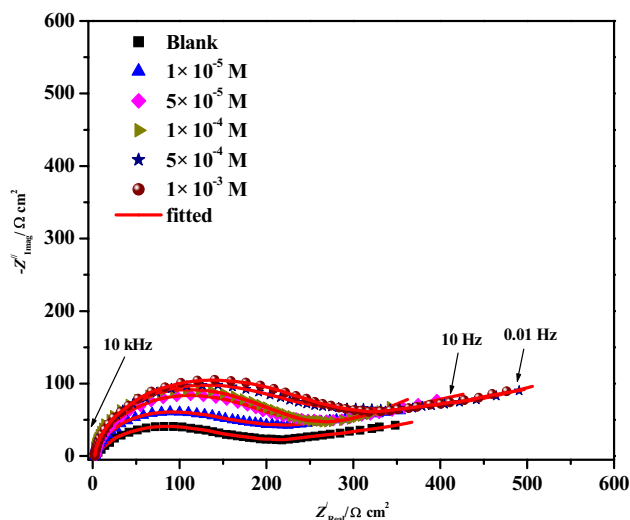


**Fig. 12** Nyquist plot for alloy III in 1 M HCl containing various concentrations of phytic acid inhibitor, measured at  $E_{corr}$  and at 25 °C

and Warburg impedance ( $Z_w$ ) increase, while the capacity of the double layer ( $C_{dl}$ ) decreases with increasing concentration of the inhibitor. This process may be argued to the inhibition of the corrosion process, i.e. hydrogen evolution and dissolution of Pb–5%In alloy as discussed above in the potentiodynamic investigation. The Warburg impedance ( $Z_w$ ) is determined from the following equations [62]:

$$Z' = \sigma \frac{1}{\omega^{1/2}} - j \frac{\sigma}{\omega^{1/2}} \quad (10)$$

$$\left| \frac{Z'}{Z''} \right| = \sqrt{2} \sigma / \omega^{1/2} \quad (11)$$

The Warburg coefficient ( $\sigma$ ) can be determined from the slope of the Warburg plot (the slope of the real parts of  $Z'$  vs.  $1/\omega^{1/2}$ ;  $\omega = 2\pi F$ ), or by fitting to an equivalent circuit modeling programs return “ $Z_w$ ” rather than  $\sigma$ ;  $Z_w$  is the Warburg impedance ( $Z_w = W$ ) calculated using the following equation:

$$\sigma = \frac{1}{Z_w \sqrt{2}} \quad (12)$$

The impedance data were interpreted according to the suitable equivalent circuit shown in Fig. 11b. This equivalent circuit was used to simulate EIS data, displaying Warburg impedance ( $Z_w$ ), in addition to solution resistance ( $R_s$ ), charge transfer resistance ( $R_{ct}$ ), and double layer capacitance ( $C_{dl}$ ) and  $C_{inhibitor}$  is the capacitance of parts that the inhibitor is adsorbed. It is observed that  $Z_w$  impedance increases with increasing the concentration of the inhibitor. This indicates that the presence of the inhibitor molecules in the solution hinders transport of species such as  $\text{Cl}^-$  ions, into the surface. Consequently, the corrosion inhibition can be attributed to the adsorption of the inhibitor molecules on the mentioned alloy surface which can block corrosion sites. Accordingly one can conclude that the values of inhibition efficiency (Table 2), obtained from Tafel extrapolation, are in agreement with those calculated from impedance (EIS) measurements at  $E_{corr}$  (Table 5).



## Surface characterization

Figure 13 shows SEM micrographs of the corrosion product formed on the surface of Pb, alloys I and V, respectively, before (Fig. 13a, e, i) and after 48 h of immersion in 1 M HCl solution in the absence (Fig. 13b, f, j) and the presence of  $1 \times 10^{-5}$  M (Fig. 13c, g, k) and  $1 \times 10^{-3}$  M (Fig. 13d, h, l) of phytic acid (PA) at 25 °C. In general, the morphology of Pb, alloy I and alloy V (Fig. 13a, e, i) is characterized by compact dense structure. The results of observed SEM in the absence of the inhibitor exhibited thick porous layer of the corrosion product (mixture from lead chloride and lead oxides in the case of pure Pb) which covered most electrode surface. However, the corrosion product formed on the surface of the investigated alloys (f and j) exhibits two layers (inner and upper layer). It is observed that the quantity of the inner layer is dense, and covering most of the surface (similar to that observed for pure Pb). But, the particles

of the upper layer are less dense, much larger in size, and the vacancies between the particles become wider so that inner layer appears easily through them. This indicates that the upper layer can be related to  $\text{InCl}_3$  or  $\text{In}_2\text{O}_3$ . However, in the solution of the lower concentration of the inhibitor ( $1 \times 10^{-5}$  M), the corrosion product is partially reduced as can be seen from the decrease of its amount (at c, g and k), whereas in the solution containing higher concentration ( $1 \times 10^{-3}$  M), almost no corrosion product is formed, particularly in the case of pure Pb (Fig. 13d). This suggests that the inhibitor is strongly adsorbed on the surface, and this hinders the corrosion process.

EDX is analytical technique used for the elemental analysis or chemical characterization of a sample. Number a in Figs. S2 and S3 (supporting data) and Fig. 14 shows EDX analysis of Pb, alloys I and V after immersion in 1 M HCl solution for 48 h in the absence of phytic acid. The data exhibited the characterization peaks related to Pb, Cl and O

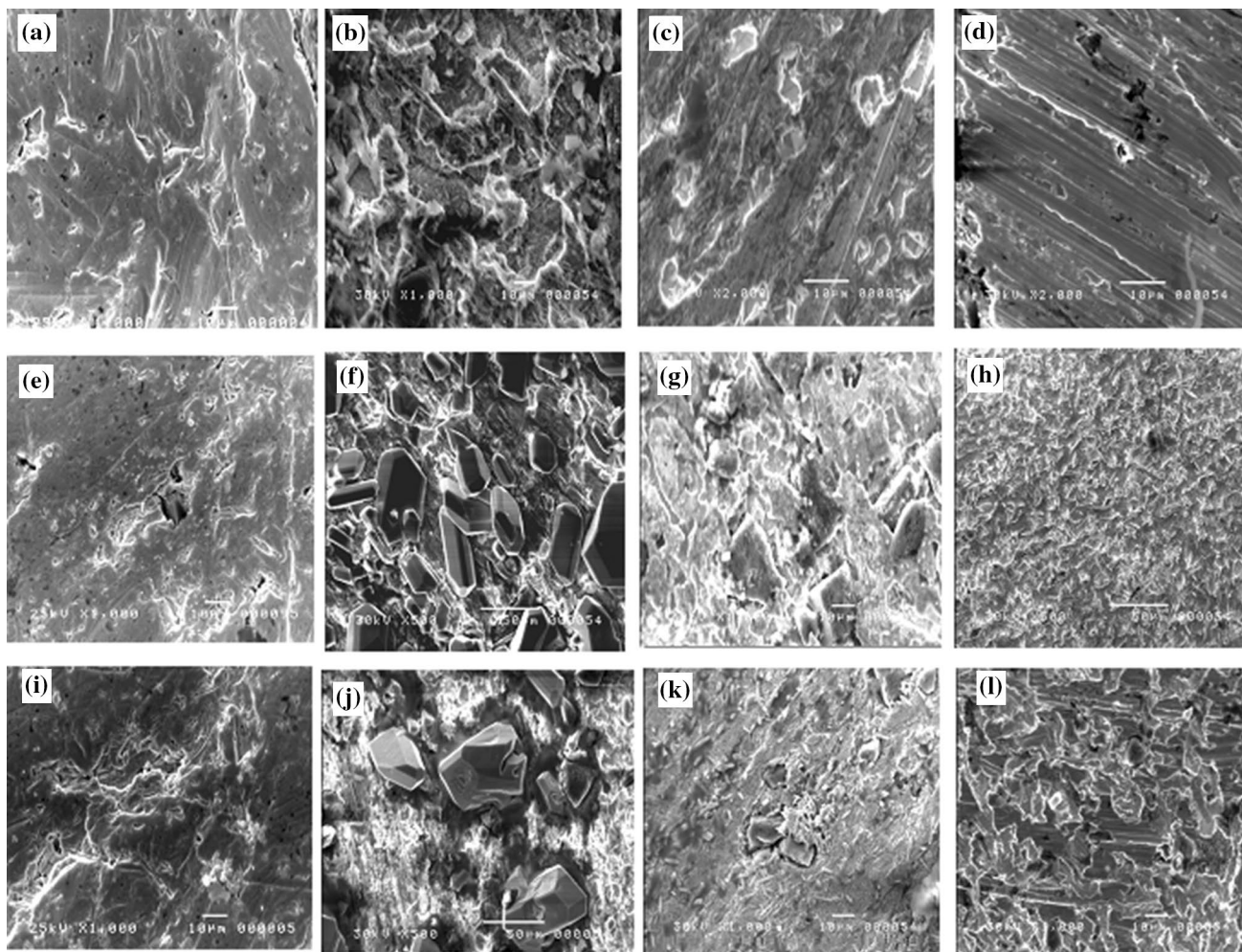


**Fig. 13** SEM micrographs of Pb, alloy I and alloy V before (a, e, i) and after immersion 48 h in 1.0 M HCl in the absence (b, f, j) and presence of  $1 \times 10^{-5}$  M (c, g, k) and  $1 \times 10^{-3}$  M (d, h, l) of phytic acid at 25 °C, respectively

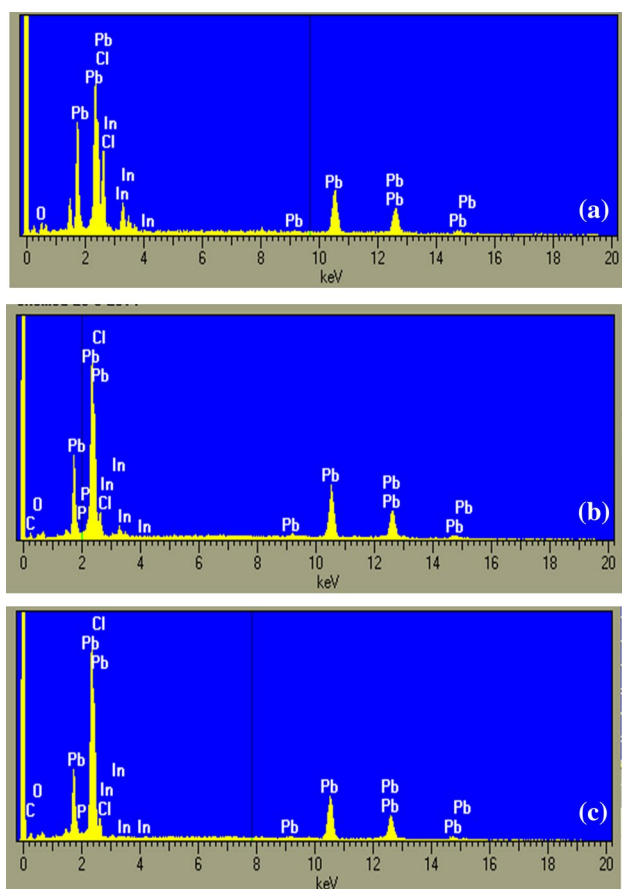


**Fig. 14** EDX analysis of alloy V after immersion in 1.0 M HCl **a** in the absence of phytic acid, **b** in the presence of  $1 \times 10^{-5}$  M and **c**  $1 \times 10^{-3}$  M phytic acid and after immersion 48 h

in the case of Pb electrode, and Pb, Cl, O and In elements for alloys. This indicates that the corrosion products on the surface of the investigated electrodes are metal chloride and metal oxide. By comparing between the quantitative analysis of Pb and its investigated alloys after the corrosion process in aggressive media without the inhibitor, it is observed that the amount of Pb element in the corrosion layer decreases

with increasing In content in the alloy. The percent of Pb element was found to be 71.03, 68.92 and 60.11% for Pb, alloys I and V, respectively (Table 6). This indicates that indium alloying with lead decreases the percent of Pb element in the corrosion product. The data in b and c of Figures S3 and S4 (supporting data) and Fig. 14 in the presence of both  $1 \times 10^{-5}$  and  $1 \times 10^{-3}$  M of phytic acid show additional peaks characteristic of C and P elements, indicating the PA molecules adsorption at the metal and alloys surfaces. The relatively high C % is due to adventitious carbon [14]. The data of EDX exhibit that Cl and O elements decrease in the presence of phytic acid. This result proved that the adsorption of inhibitor molecules on the surface of pure Pb and its studied alloys decreases metal chloride and its oxide (corrosion product), but higher concentration ( $1 \times 10^{-3}$  M) significantly reduces the corrosion layer. The percentages of the elements present on the analyzed surfaces with and without the studied inhibitor are calculated and mentioned in Table 6. Consequently, the obtained data of EDX in addition to SEM micrographs support the results obtained by both potentiodynamic polarization and EIS measurements.

## Conclusions

In the present study, electrochemical methods including potentiodynamic polarization and electrochemical impedance spectroscopy (EIS) measurements have been used to elucidate the corrosion and corrosion inhibition of Pb and Pb–In alloys in HCl solution. Also, some supplementary experiments like SEM and EDX have been carried out to confirm the electrochemical results. The following conclusions can be drawn from this study:

1. It was demonstrated that phytic acid is an efficient corrosion inhibitor for Pb and Pb–In alloys in 1.0 M HCl solution, and the inhibition efficiency increases with increasing the inhibitor concentration and decreases with increasing the reaction temperature, the  $\eta$  % being

**Table 6** Elements of Pb and Pb–In alloys substrates after immersion in 1.0 M HCl solution in the absence and presence of phytic acid obtained from EDX analyzed by % weight with an accuracy  $\pm 5.0\%$

Test	Sample's name	Elements (wt.%)					
		Pb	In	O	Cl	P	C
In the absence of phytic acid	Pb	71.03	–	20.96	8.01	–	–
	Alloy I	68.92	0.75	10.96	19.37	–	–
	Alloy V	60.11	17.28	6.37	16.24	–	–
In the presence of $1 \times 10^{-5}$ M phytic acid	Pb	81.53	–	0.22	8.60	0.71	8.93
	Alloy I	88.59	0.05	1.40	3.55	0.68	5.82
	Alloy V	80.08	6.92	0.43	5.26	0.73	7.44
In the presence of $1 \times 10^{-3}$ M phytic acid	Pb	93.79	–	0.44	1.11	1.02	4.52
	Alloy I	90.17	0.80	1.42	3.49	0.68	3.44
	Alloy V	85.32	1.05	0.06	3.67	0.91	9.11

in the range 72–79.2% at  $10^{-3}$  M and 25 °C. However, the inhibition efficiency in the case of pure Pb is higher than that of its investigated alloys at lower concentration ( $10^{-5}$  M), which is due to less active sites on the surface of alloys, leading to less adsorption of inhibitor molecules.

- Phytic acid inhibits both anodic and cathodic reactions by adsorption on the metal and alloys surfaces and hence behaves like mixed-type inhibitor.
- The impedance spectra recorded for pure Pb and its studied alloys (except alloy III, 5% In) in the absence and presence of various concentrations of the inhibitor, display one capacitive loop. However, alloy III exhibits different behavior to that observed of the other investigated alloys; one capacitive loop at higher frequency followed by the Warburg tail at lower frequency is observed. This anomalous behavior of this alloy (5% In) can be attributed to that the surface becomes more heterogeneous; consequently, the diffusion of soluble species from the alloy surface to the bulk of solution is easier.
- Langmuir adsorption model fits well with the experimental data and regarded as physical adsorption. Moreover,  $\Delta H_{\text{ads}}^0$ ,  $\Delta S_{\text{ads}}^0$  and  $\Delta G_{\text{ads}}^0$  were evaluated and interpreted. The calculated values of  $\Delta H_{\text{ads}}^0$  and  $\Delta G_{\text{ads}}^0$  are negative, while those for  $\Delta S_{\text{ads}}^0$  are positive.
- SEM micrographs and EDX revealed that the corroded surface area is decreased with increasing concentration of the inhibitor.

**Open Access** This article is distributed under the terms of the Creative Commons Attribution 4.0 International License (<http://creativecommons.org/licenses/by/4.0/>), which permits unrestricted use, distribution, and reproduction in any medium, provided you give appropriate credit to the original author(s) and the source, provide a link to the Creative Commons license, and indicate if changes were made.

## References

- Cao F, Wei J, Dong J, Ke W (2018) The corrosion inhibition effect of phytic acid on 20SiMn steel in saturated  $\text{Ca}(\text{OH})_2$  solution with  $1 \text{ mol L}^{-1}$  NaCl. *Corros Eng Sci Technol* 53:283–292
- Finsgar M, Fassbender S, Nicolini F, Milosev I (2009) Polyethyleneimine as a corrosion inhibitor for ASTM 420 stainless steel in near-neutral saline media. *Corros Sci* 51:525–533
- Shimizu K (1988) The lead/acid battery industry in Japan. *J Power Sour* 23:33–46
- Kiani MA, Mousavi MF, Ghasemi S, Shamsipur M, Kazemi SH (2008) Inhibitory effect of some amino acids on corrosion of Pb–Ca–Sn alloy in sulfuric acid solution. *Corros Sci* 50:1035–1045
- El-Sayed A, El-Shikh EMI, Mohran HS, Esmail M, Shelkamy HA (2015) Effect of indium alloying with lead on the mechanical properties and corrosion resistance of lead–indium alloys in sulfuric acid solution. *Mett Mat Trans A* 46:1995–2006
- Abd El Wanees S, Abd El Aal EE (2010) N-Phenylcinnamimide and some of its derivatives as inhibitors for corrosion of lead in HCl solutions. *Corros Sci* 52:338–344
- Ju H, Kai ZP, Li Y (2008) Aminic nitrogen-bearing polydentate Schiff base compounds as corrosion inhibitors for iron in acidic media: a quantum chemical calculation. *Corros Sci* 50:865–871
- Scendo M (2008) The influence of adenine on corrosion of copper in chloride solutions. *Corros Sci* 50:2070–2077
- El-Sayed A, Shaker AM, Abd El-Lateef HM (2010) Corrosion inhibition of tin, indium and tin–indium alloys by adenine or adenosine in hydrochloric acid solution. *Corros Sci* 52:72–81
- El-Sayed A, Mohran HS, Abd El-Lateef HM (2010) The inhibition effect of 2,4,6-tris (2-pyridyl)-1,3,5-triazine on corrosion of tin, indium and tin–indium alloys in hydrochloric acid solution. *Corros Sci* 52:1976–1984
- Hammouti B, Salghi R, Kertit S (1998) Electrochemical behaviour of lead in 0.3 M HCl in presence of pyrazolic. *J Electrochem Soc India* 47:31–34
- Helal NH, El-Rabee MM, Abd El-Hafez GhM, Badawy WA (2008) Environmentally safe corrosion inhibition of Pb in aqueous solutions. *J Alloys Compd* 456:372–378
- Badway WA, Hefny MM, El-Agamy SS (1990) Effect of some organic amines as corrosion inhibitors for lead in 0.3 M HCl solution. *Corrosion* 46:978–982
- Dus And B, Smialovska ZS (1972) Effect of some phosphoroorganic compounds on the corrosion rate of various metals in acid solutions. *Corrosion* 28:105–114
- Peca D, Pihlar B, Ingrid M (2014) Protection of copper surface with phytic acid against corrosion in chloride solution. *Acta Chim Slov* 61:457–467
- Wang Y-H, He J-B (2012) Corrosion inhibition of copper by sodium phytate in NaOH solution: cyclic voltabsorptometry for in situ monitoring of soluble corrosion products. *Electrochim Acta* 66:45–51
- Yang HF, Yang Y, Liu H, Zhang ZR, Shen GL, Yu RQ (2005) Formation of inositol hex phosphate monolayers at the copper surface from a Na-salt of phytic acid solution studied by in situ surface enhanced Raman scattering spectroscopy, Raman mapping and polarization measurement. *Anal Chim Acta* 548:159–165
- Yang HF, Feng J, Liu YL, Yang Y, Zhang ZR, Shen GL, Yu RQ (2004) Electrochemical and surface enhanced Raman scattering spectroelectrochemical study of phytic acid on the silver electrode. *J Phys Chem B* 108:17412–17417
- Zhang R, Yang HF, Sun YP, Song W, Zhu X, Wang N, Wang Y, Pan YC, Zhang ZR (2009) Competitive adsorption of 4-methyl-4H-1,2,4-triazole-3-thiol and Na salt of phytic acid on a silver surface: Raman spectral and electrochemical observations. *J Phys Chem C* 113:9748–9754
- Hao C, Yin RH, Wan ZY, Xu QJ, Zhou GD (2008) Electrochemical and photo electrochemical study of the self-assembled monolayer phytic acid on cupro nickel B30. *Corros Sci* 50:3527–3533
- El-Sayed A, Harm U, Mangold KM, Furbeth W (2012) Protection of galvanized steel from corrosion in NaCl solution by coverage with phytic acid SAM modified with some cations and thiols. *Corros Sci* 55:339–350
- El-Sayed A, Shaker AM, Gad El-Kareem H (2003) Anodic behaviour of antimony and antimony–tin alloys in alkaline solutions. *Bull Chem Soc Jpn* 76:1527–1535
- Abd El-Rehim SS, Hassan HH, Mohamed NF (2004) Anodic behaviour of tin in maleic acid solution and the effect of some inorganic inhibitors. *Corros Sci* 46:1071–1082
- El-Sayed A, Mohran HS, Abd El-Lateef HM (2011) Inhibitive action of ferricyanide complex anion on both corrosion and



- passivation of zinc and zinc–nickel alloy in the alkaline solution. *J Power Sources* 196:6573–6582
25. Mohran HS, El-Sayed A, Abd El-Lateef HM (2009) Hydrogen evolution reaction on Sn, In, and Sn–In alloys in carboxylic acids. *J Solid State Electrochem* 13:1147–1155
  26. Tremont R, De Jesus-Cardona H, Garcia-Orozco J, Castro RJ, Cabrera CR (2000) 3-Mercaptopropyltrimethoxysilane as a Cu corrosion inhibitor in KCl solution. *J Appl Electrochem* 30:737–743
  27. Schultze JW, Wippermann K (1987) Inhibition of electrode processes on copper by AHT in acid solutions. *Electrochim Acta* 32:823–831
  28. Abdel Aal MS, Abdel Wahab AA, El-Saied A (1981) A study of the inhibiting action of benzene thiols and related compounds on the corrosion of zinc in acidic media. *Corrosion* 37:557–563
  29. El-Sayed A, Mohran HS, Shalkami HA (2014) Role of indium alloying with lead as a means to reduce the passivation phenomena in lead/acid batteries. *Int J Electrochem* 2014:16
  30. Antropov LI (1972) Theoretical electrochemistry. MIR Publications, Moscow, p 276
  31. Antropov LI (1967) A correlation between kinetics of corrosion and the mechanism of inhibition by organic compounds. *Corros Sci* 7:607–620
  32. El-Sayed A (1998) The inhibition effect of some nitrogen-heterocyclic compounds on corrosion of aluminium and its alloys in HCl solution. *J Electrochem Soc Jpn (DENKI KAGAKU)* 66:176–185
  33. Vani R, Praveen BM, Kumar G (2015) Polyethylene glycol as a corrosion inhibitor for lead and lead free solders in acidic medium. *Int J Mech Eng Rob Res* 4:120–135
  34. Amin MA, Ibrahim MM (2011) Corrosion and corrosion control of mild steel in concentrated H<sub>2</sub>SO<sub>4</sub> solutions by a newly synthesized glycine derivative. *Corros Sci* 53:873–885
  35. Aouine Y, Sfaira M, Ebn Touhami M, Alami A, Hammouti B, Elbakri M, El Hallaoui A, Tourir R (2012) Temperature and time investigations on the adsorption behavior of isoindoline, tetrazole and isoindoline–tetrazole on corrosion of mild steel in acidic medium. *Int J Electrochem Sci* 7:5400–5419
  36. Hassan HH (2007) Inhibition of mild steel corrosion in hydrochloric acid solution by triazole derivatives: part II: time and temperature effects and thermodynamic treatments. *Electrochim Acta* 53:1722–1730
  37. Amin MA, Abd El-Rehim SS, El-Sherbini EEF, Bayomi RS (2007) The inhibition of low carbon steel corrosion in hydrochloric acid solutions by succinic acid: Part I. Weight loss, polarization, EIS, PZC, EDX and SEM studies. *Electrochim Acta* 52:3588–3600
  38. Bentiss F, Lebrini M, Lagrenee M (2005) Thermodynamic characterization of metal dissolution and inhibitor adsorption processes in mild steel/2,5-bis (n-thienyl)-1,3,4-thiadiazoles/hydrochloric acid system. *Corros Sci* 47:2915–2931
  39. Babic- Samardzija K, Khaled KF, Hackerman N (2005) Investigation of the inhibiting action of O-, S- and N-dithiocarbamate(1,4,8,11-tetraazacyclotetradecane) cobalt(III) complexes on the corrosion of iron in HClO<sub>4</sub> acid. *Appl Surf Sci* 240:327–340
  40. Sahin M, Bilgic S, Yilmaz H (2002) The inhibition effects of some cyclic nitrogen compounds on the corrosion of the steel in NaCl mediums. *Appl Surf Sci* 195:1–7
  41. Abd El-Lateef HM, Mohamed Adam SS, Khalaf MM (2018) Synthesis of polar unique 3D metal-imine complexes of salicylidene anthranilate sodium salt. Homogeneous catalytic and corrosion inhibition performance. *J Taiwan Inst Chem Eng* 88:286–304
  42. Obot IB, Egbedi NO (2009) Ipomoea involcrata as an eco-friendly inhibitor for aluminium in alkaline medium. *Electrochim Acta* 27:517–524
  43. Tang F, Wang X, Xu X, Li L (2010) Phytic acid doped nanoparticles for green anticorrosion coatings. *Colloids Surf A* 369:101–105
  44. Adam MSS, Abd El-Lateef HM, Soliman KA (2018) Anionic oxide vanadium Schiff base amino acid complexes as potent inhibitors and as effective catalysts for sulfides oxidation: experimental studies complemented with quantum chemical calculations. *J Mol Liq* 250:307–322
  45. Abd El-Lateef HM, Abbasov VM, Aliyeva LI, Qasimov EE, Ismayilov IT (2013) Inhibition of carbon steel corrosion in CO<sub>2</sub>-saturated brine using some newly surfactants based on palm oil: experimental and theoretical investigations. *Mater Chem Phys* 142:502–512
  46. Refay SA, Taha F, Abd El-Malak AM (2004) Inhibition of stainless steel pitting corrosion in acidic medium by 2 mercaptobenzoxazole. *Appl Surf Sci* 236:175–185
  47. Abd El-Lateef HM, Tantawy AH (2016) Synthesis and evaluation of novel series of Schiff base cationic surfactants as corrosion inhibitors for carbon steel in acidic/chloride media: experimental and theoretical investigations. *RSC Adv* 6:8681–8700
  48. Abd El-Lateef HM (2015) Experimental and computational investigation on the corrosion inhibition characteristics of mild steel by some novel synthesized imines in hydrochloric acid solutions. *Corros Sci* 92:104–117
  49. Solomon MM, Gerengi H, Umoren SA (2017) Carboxymethyl cellulose/silver nanoparticles composite: synthesis, characterization and application as a benign corrosion inhibitor for St37 Steel in 15% H<sub>2</sub>SO<sub>4</sub> medium. *ACS Appl Mater Interfaces* 9(7):6376–6389
  50. Noor EA, Al-Moubaraki AH (2008) Thermodynamic study of metal corrosion and inhibitor adsorption processes in mild steel/1-methyl-4[4(-X)-styryl pyridinium iodides/hydrochloric acid systems. *Mater Chem Phys* 110:145–154
  51. Solomon MM, Gerengi H, Umoren SA (2017) Carboxymethyl cellulose/silver nanoparticles composite: synthesis, characterization and application as a benign corrosion inhibitor for St37 Steel in 15% H<sub>2</sub>SO<sub>4</sub> medium. *CS Appl Mater Interfaces* 9(7):6376–6389
  52. El-Sherif RM, Badawy WA (2011) Mechanism of corrosion and corrosion inhibition of tin in aqueous solutions containing tartaric acid. *Int J Electrochem Sci* 6:6469–6482
  53. Badawy WA, Al-Kharafi FM, El-Azab AS (1999) Electrochemical behaviour and corrosion inhibition of Al, Al-6061 and Al–Cu in neutral aqueous solutions. *Corros Sci* 41:709–727
  54. Ansari KR, Yadav DK, Ebenso EE, Quraishi MA (2012) Novel and effective pyridyl substituted 1, 2, 4-triazole as corrosion inhibitor for mild steel in acid solution. *Int J Electrochem Sci* 7:4780–4799
  55. Yadav DK, Chauhan DS, Ahamad I, Quraishi MA (2013) Electrochemical behavior of steel/acid interface: adsorption and inhibition effect of oligomeric aniline. *RSC Adv* 3:632–646
  56. Abd El-Lateef HM, Abu-Dief AM, Abdel-Rahman LH, Saudo EC, Aliaga-Alcalde N (2015) Electrochemical and theoretical quantum approaches on the inhibition of C1018 carbon steel corrosion in acidic medium containing chloride using some newly synthesized phenolic Schiff bases compounds. *J Electroanal Chem* 743:120–133
  57. Kh Ismail M, El-Moneim AA, Badawy WA (2001) Stability of sputter-deposited amorphous Mn–Ta alloys in chloride-free and chloride-containing H<sub>2</sub>SO<sub>4</sub> solutions. *J Electrochem Soc* 148:C81–C87





58. Khaled KF (2003) The inhibition of benzimidazole derivatives on corrosion of iron in 1 M HCl solutions. *Electrochim Acta* 48:2493–2503
59. Hleli S, Abdelghani A, Tlili A (2003) Impedance spectroscopy technique for DNA hybridization. *Sensors* 3:472–479
60. Babic-Samardzija K, Khaled KF, Hackerman N (2005) Heterocyclic amines and derivatives as corrosion inhibitors for iron in perchloric acid. *Anti-Corros Methods Mater* 52:11–21
61. El-Sayed A, Mohran HS, Abd El-Lateef HM (2010) Effect of minor nickel alloying with zinc on the electrochemical and corrosion behavior of zinc in alkaline solution. *J Power Sources* 195:6924–6936
62. Abd El-Lateef HM, El-Sayed A, Mohran HS (2015) Role of Ni content in improvement of corrosion resistance of Zn–Ni alloy in 3.5% NaCl solution. Part I: polarization and impedance studies. *Trans Nonferrous Met Soc China* 25:2807–2816

**Publisher's Note** Springer Nature remains neutral with regard to jurisdictional claims in published maps and institutional affiliations.

